ORIGINAL ARTICLE

CrossMark

RANKL Signaling Sustains Primary Tumor Growth in Genetically Engineered Mouse Models of Lung Adenocarcinoma

Julien Faget, PhD,[a] Caroline Contat, MS,[a] Nadine Zangger, PhD,[a,b]
Solange Peters, MD, PhD,[c] Etienne Meylan, PhD[a,*]

[a]Swiss Institute for Experimental Cancer Research, School of Life Sciences, Ecole Polytechnique Fédérale de Lausanne, Lausanne, Switzerland
[b]Bioinformatics Core Facility, Swiss Institute of Bioinformatics, Lausanne, Switzerland
[c]Department of Oncology, Centre Hospitalier Universitaire Vaudois, University of Lausanne, Lausanne, Switzerland

ABSTRACT

Introduction: NSCLC is the leading cause of cancer mortality. Recent retrospective clinical analyses suggest that blocking the receptor activator of NF-κB (RANK) signaling pathway inhibits the growth of NSCLC and might represent a new treatment strategy.

Methods: Receptor activator of NF-κB gene (RANK) and receptor activator of NF-κB ligand gene (RANKL) expression in human lung adenocarcinoma was interrogated from publicly available gene expression data sets. Several genetically engineered mouse models were used to evaluate treatment efficacy of RANK-Fc to block RANKL, with primary tumor growth measured longitudinally using microcomputed tomography. A combination of RANKL blockade with cisplatin was tested to mirror an ongoing clinical trial.

Results: In human lung adenocarcinoma data sets, RANKL expression was associated with decreased survival and KRAS mutation, with the highest levels in tumors with co-occurring KRAS and liver kinase B1 gene (LKB1) mutations. In $Kras^{LSL-G12D/WT}$, $Kras^{LSL-G12D/WT}$; $Lkb1^{Flox/Flox}$ and $Kras^{LSL-G12D/WT}$; $p53^{Flox/Flox}$ mouse models of lung adenocarcinoma, we monitored an impaired progression of tumors upon RANKL blockade. Despite elevated expression of RANKL and RANK in immune cells, treatment response was not associated with major changes in the tumor immune microenvironment. Combined RANK-Fc with cisplatin revealed increased efficacy compared with that of single agents in p53- but not in Lkb1-deficient tumors.

Conclusions: RANKL blocking agents impair the growth of primary lung tumors in several mouse models of lung adenocarcinoma and suggest that patients with KRAS-mutant lung tumors will benefit from such treatments.

Introduction

With more than 1.5 million deaths yearly, lung cancer has become the leading cause of cancer-related mortality worldwide, with NSCLC representing 80% to 85% of cases.[1] Although new therapies are emerging to combat lung adenocarcinoma, which is the main histological subtype of NSCLC, their use is currently limited to a subset of molecularly selected patients, and no specific targeted therapy has demonstrated activity against tumors carrying the most frequently mutated proto-oncogene, KRAS.[2] One interesting approach for cancer treatment is

to identify actionable membrane-bound or secreted ligand-receptor systems that act in the tumor environment to promote disease progression, which can be very selectively blocked through the use of small compounds or antibodies. One such example is the tumor necrosis factor (TNF) family member, receptor activator of NF-κB (RANK) ligand (RANKL) that signals through its receptor RANK, which was first discovered for communication between T cells and dendritic cells.[3] Through its receptor RANK, RANKL activates osteoclasts for bone resorption, promotes lymphocyte maturation and function, and enables mammary gland and secondary lymph node organogenesis.[4–6] A link between RANKL signaling and cancer has been established in recent years: first, and perhaps owing to its bone remodeling capabilities, the RANKL-RANK pathway facilitates bone metastasis formation[7,8]; second, it promotes seeding of breast tumor cells into the lungs in a T-regulatory–cell-dependent manner[9]; third, it participates in development of progestin-dependent mammary tumors.[10,11] The importance of this signaling pathway in primary breast cancer is well documented, with *RANKL* mRNA being stabilized in response to progesterone, leading to increased RANKL protein expression that promotes tumor cell proliferation[12] and epithelial-

mesenchymal transition to foster tumor cell migration.[13] In contrast, much less is known about its contribution in primary tumors from other carcinomas such as lung cancer. Recently, in a large international clinical trial of patients with advanced solid tumors (excluding breast and prostate cancer) or multiple myeloma, denosumab, a fully human monoclonal antibody that binds RANKL and blocks RANKL-RANK interaction, demonstrated activity in preventing bone metastasis–related adverse events, such as fracture or the need for radiotherapy. Although this trial failed to reveal any difference in overall survival (OS),[14] a retrospective subgroup analysis from this trial reported increased OS specifically in patients with NSCLC.[15,16] In our study, we sought to investigate the involvement of RANKL in primary tumors from NSCLC by using genetically engineered mouse models.

## Material and Methods

Animal Models

K-$ras^{LSL\text{-}G12D/WT}$ (K) and $p53^{FL/FL}$ mice in a C57BL6/J background were purchased from The Jackson Laboratory (Bar Harbor, ME) and bred together to obtain K-$ras^{LSL\text{-}G12D/WT}$; $p53^{FL/FL}$ (KP) mice. $Lkb1^{FL/FL}$ mice in a mixed background (FVB; 129S6) were obtained from R.
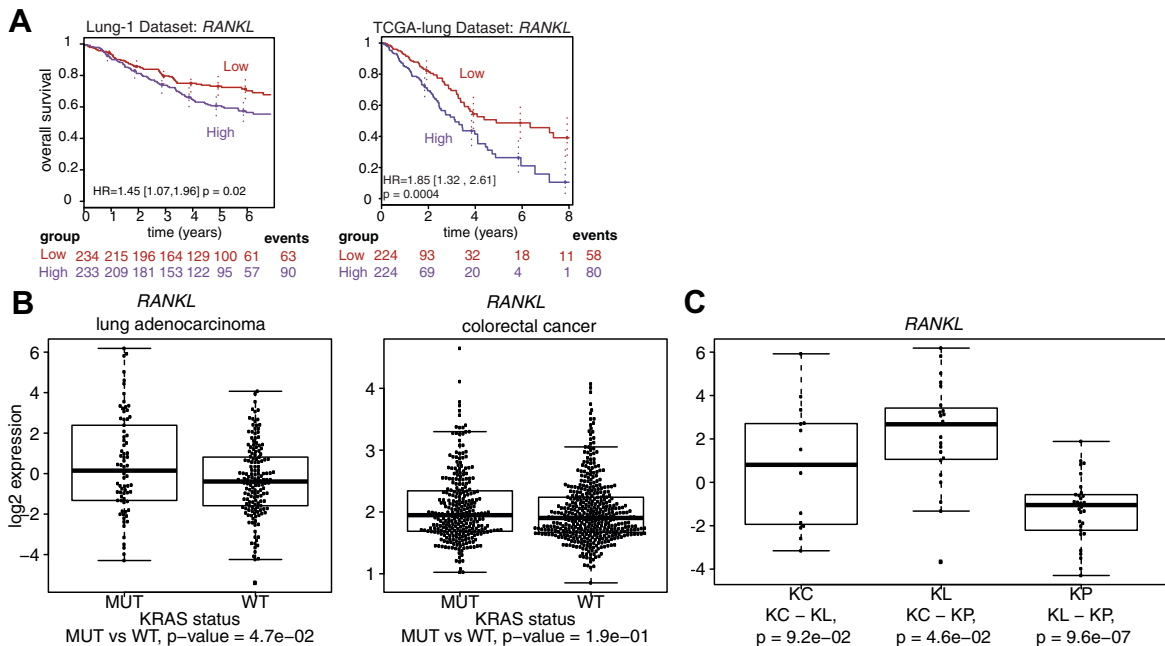
Figure 1. Receptor activator of NF-κB ligand gene (*RANKL*) expression correlates with poor overall survival and *KRAS* mutation in human lung adenocarcinoma. (*A*) Kaplan-Meier curves for overall survival, hazard ratios (HRs), confidence intervals, and *p* values of pairwise differences between groups with high or low *RANKL* expression in the Lung-1 (*left*) and The Cancer Genome Atlas (TCGA) lung adenocarcinoma (*right*) data sets. Differences between curves were assessed by using the log rank test (Mantel-Cox). (*B*) *RANKL* expression level (log2) in the TCGA lung (*left*) and Pan-European Trial in Adjuvant Colon Cancer (*right*) data sets split into two groups based on *KRAS* mutation status (TCGA lung: mutated [MUT], n = 60; wild type [WT], n = 138; Pan-European Trial in Adjuvant Colon Cancer: MUT, n = 283; WT, n = 425). Statistical analyses were performed by using Kruskal-Wallis test. (*C*) *RANKL* expression level (log2) in mutant for *KRAS* and enriched for *CDKN2A* mutations (KC), mutant for *KRAS* and enriched for liver kinase B1 gene (*LKB1*) mutations (KL), and mutant for *KRAS* and enriched for tumor protein p53 gene (*TP53*) mutations (KP) clusters as defined in Skoulidis et al.[18] *p* Values are indicated. Statistical analyses were performed by using the Kruskal-Wallis test.
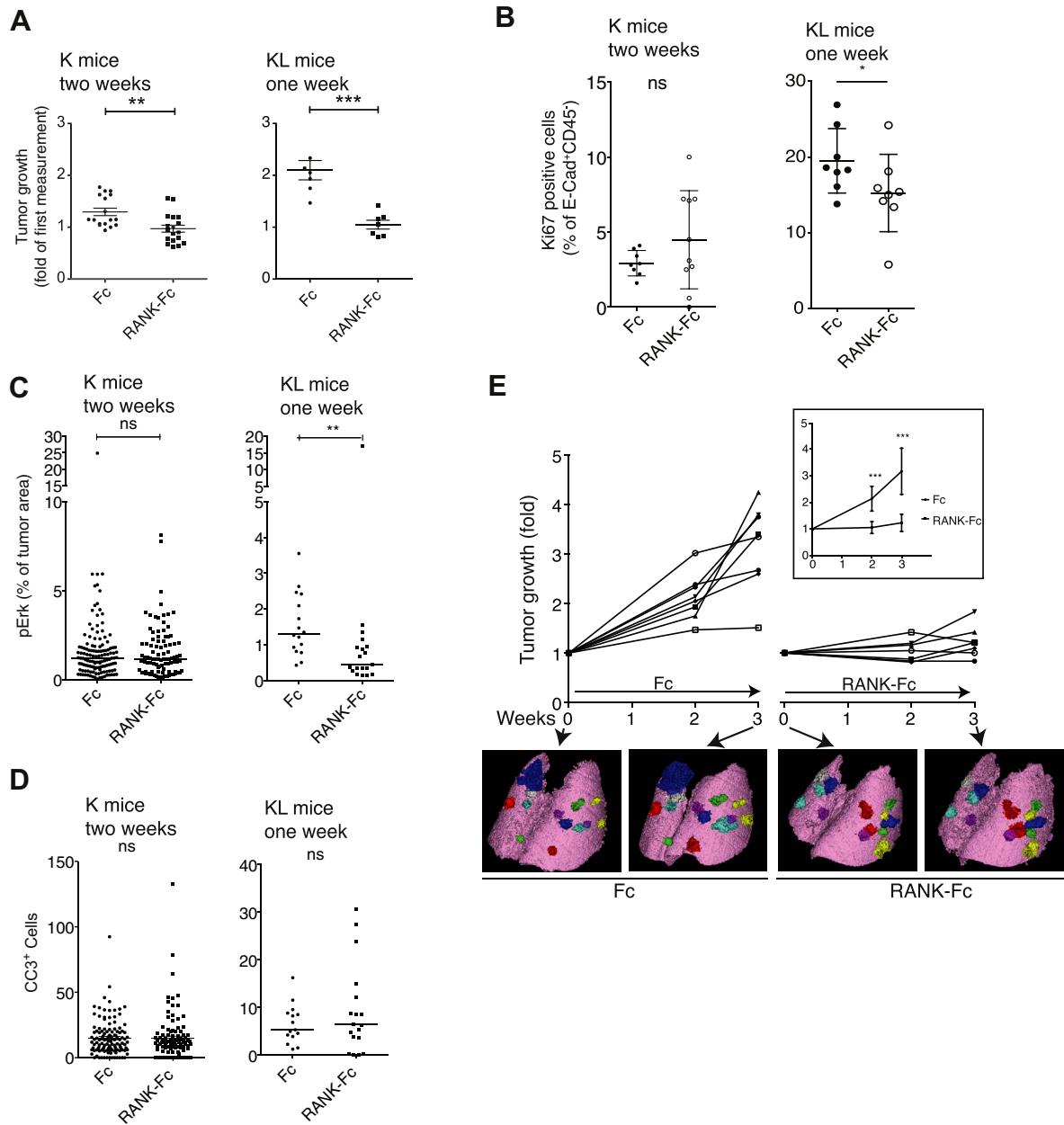
Figure 2. Receptor activator of NF-κB (RANK) ligand blockade inhibits the growth of lung tumors in $Kras^{LSL-G12D/WT}$ and $Kras^{LSL-G12D/WT}$; $Lkb1^{FL/FL}$ mice. (*A*) Dot plots represent tumor growth, as measured by microcomputed tomography (μCT), between initiation and end of treatment, in control Fc or RANK-Fc treated K-$ras^{LSL-G12D/WT}$ (K) (n = 17 versus 18) and $Kras^{LSL-G12D/WT}$; $Lkb1^{FL/FL}$ (KL) (n = 7 versus 7) mouse models. Treatment started at 23 and 18 weeks after tumor initiation, respectively, and treatment duration is indicated. (*B*) Dot plot shows the percentage of Ki67-positive cells among E-caderin-positive, CD45-negative viable tumor cells from K (*left*) or KL (*right*) tumors after treatment with control Fc (K: n = 8; KL: n = 8) or RANK-Fc (K: n = 10; KL: n = 8). (*C*) Dot plots represent the percentage of phospho-Erk (pErk)-positive area per lesion in K or KL mice treated with control-Fc (K: n = 131; KL: n = 16) or RANK-Fc (K: n = 95; KL: n = 19). (*D*) Dot plots show number of cleaved caspase-3–positive cells per 10^6 pixels on lung tumor sections scanned at $\times$400. K (*left*) or KL (*right*) mice treated with control-Fc (K: n = 123; KL: n = 15) or RANK-Fc (K: n = 103; KL: n = 18). (*E*) Tumor growth monitoring by μCT over a 3-week period. KL mice were treated with control Fc or RANK-Fc. Eight and seven tumors were monitored for Fc or RANK-Fc treatment, respectively. Curves represent volume evolution of each tumor, as fold of the first measurement. μCT imaging was done at weeks 0, 2, and 3 of treatment. Means with SE of the mean are shown in the box. μCT images show lungs and the detectable tumors of two representative mice at weeks 0 and 3 of treatment. (*A-E*) Statistical analyses were performed by using the Mann-Whitney test; asterisks show *p* values: *p < 0.05, **p < 0.01, ***p < 0.001. ns, not significant.
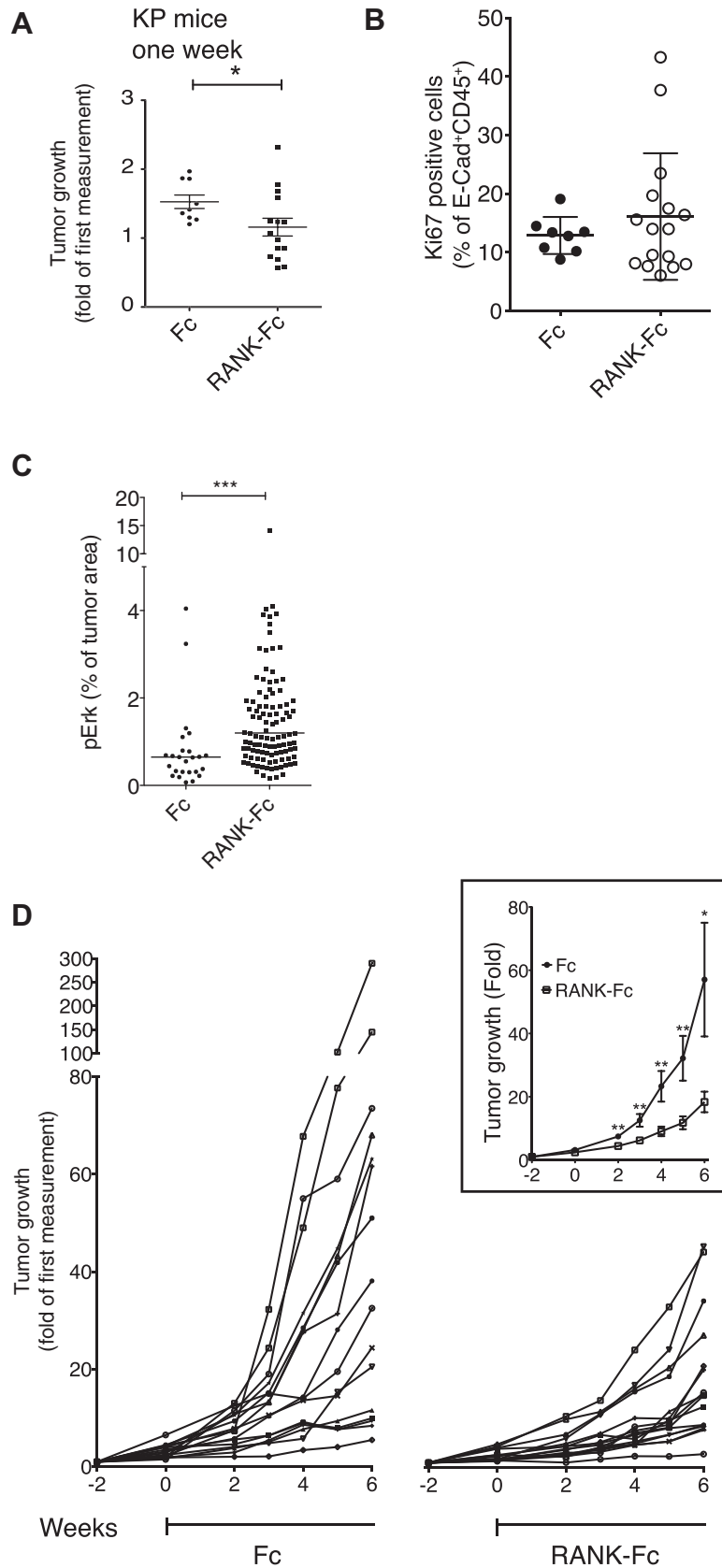
Figure 3. Receptor activator of NF-κB (RANK) ligand blockade elicits long-term antitumor response in $Kras^{LSL-G12D/WT}$; $p53^{FL/FL}$ mice. (*A*) Dot plots represent tumor growth, as measured by microcomputed tomography (μCT), between initiation and end of treatment, in control Fc or RANK-Fc treated $Kras^{LSL-G12D/WT}$; $p53^{FL/FL}$ (KP) mice (n = 9 versus 15). Treatment started at 13 weeks after tumor initiation and lasted 1 week. (*B*) Dot plot represents the percentage of Ki67-positive cells among the

DePinho (The University of Texas M. D. Anderson Cancer Center, Houston, Texas) through the National Cancer Institute mouse repository, backcrossed seven times to C57BL6/J, and bred with $K\text{-}ras^{LSL\text{-}G12D/WT}$ mice to obtain $K\text{-}ras^{LSL\text{-}G12D/WT}$; $Lkb1^{FL/FL}$ (KL) mice.

Mouse Treatment Modalities

Recombinant RANK (mouse):Fc (human) fusion and human Fc immunoglobulin G1 control proteins were purchased from AdipoGen Life Sciences (Liestal, Switzerland). Mice were treated with 10 mg/kg of RANK-Fc or Fc control by subcutaneous injection twice weekly. Cisplatin was used at 3.5 mg/kg in sterile phosphate-buffered saline by intraperitoneal injection.

Study Approval

All mouse experiments were performed with permission of the Veterinary Authority of the Canton de Vaud, Switzerland (license number VD2391).

Results and Discussion

RANKL Expression Correlates with Poor OS and KRAS Mutation in Lung Adenocarcinoma

To test the hypothesis that RANKL signaling regulates the development of primary lung tumors, we interrogated two independent publicly available gene expression data sets of human lung adenocarcinoma, and one of colorectal cancer (CRC). It revealed that high expression of *RANKL* (also known as TNF superfamily member 11 gene [*TNFSF11*]) was associated with a reduced OS compared with that of tumor samples with low expression in lung adenocarcinoma but not in CRC. *RANK* (also known as TNF receptor superfamily member 11A [*TNFRSF11A*]) expression was also associated with reduced OS, but only in one of the two lung data sets, whereas it was linked with better OS for patients with CRC (Fig. 1*A* and Supplementary Fig. 1*A–D*), suggesting a peculiar relationship between RANK/RANKL signaling and lung cancer progression that is not shared by CRC. Specific data analysis from The Cancer Genome Atlas (TCGA [https://tcga-data.nci.nih.gov/tcga/]) also showed that *RANKL* expression was significantly stronger in *KRAS*-mutant than in *KRAS* wild-type (WT) tumors in lung adenocarcinoma but not in CRC (Fig. 1*B*). *KRAS* mutation itself in lung adenocarcinoma is not prognostic of poor OS as reported earlier[17] (Supplementary Fig. 1*E*). Recently, gene expression analysis from TCGA enabled to define biologically distinct *KRAS*-mutant lung tumors in function of co-occurring mutations in tumor suppressors.[18] Specifically, this analysis highlighted three different subgroups, called *KC* (mutant for *KRAS* and enriched for *CDKN2A* mutations), *KP* (mutant for *KRAS* and enriched for *TP53* mutations), and *KL* (mutant for *KRAS* and enriched for liver kinase B1 gene [*LKB1*] mutations). Analogies were drawn between cluster-specific biological signatures and tumors from different mouse models of oncogenic *Kras*-dependent lung tumorigenesis. For example, gene set enrichment analysis of the KL cluster retrieved gene signatures obtained from murine lung tumors expressing mutant *Kras(G12D)* and deficient for *Lkb1*.[18] Intrigued by these analogies, we decided to compare *RANKL* expression between each cluster. This analysis showed that *RANKL* levels are significantly higher in the KL cluster than in the KP cluster ($p = 9.6e\text{-}07$ [Fig. 1*C*]). From each of the *KRAS*-mutant and *KRAS* WT group, as well as from the KC, KL, and KP clusters from *KRAS*-mutant tumors, we interrogated the genes most positively correlated with RANKL (Supplementary Table 1). This analysis revealed hallmark pathways of cell cycle, mammalian target of rapamycin signaling, epithelial-mesenchymal transition (EMT), hypoxia, and glycolysis in the *KRAS*-mutant samples. In contrast, *RANKL*-correlated genes in *KRAS* WT tumor samples revealed pathways representing EMT, inflammatory and angiogenic responses, and interestingly, KRAS signaling. *KRAS*-mutant subgroup analysis highlighted further differences between the clusters, with enrichments for pathways of cell cycle and EMT in KC; cell cycle and mammalian target of rapamycin signaling in KL; and inflammatory and immune responses, KRAS signaling, and EMT in KP (see Supplementary Table 1). Thus, *RANKL* expression, which is stronger in *KRAS*-mutant samples than in *KRAS* WT samples, is associated with poor OS in human lung adenocarcinoma. Within *KRAS*-mutant tumors, expression of *RANKL* is the strongest in a subgroup of tumors harboring *LKB1* mutations.

Pharmacological Blockade of Rankl Inhibits Tumor Growth in Mouse Models of Lung Adenocarcinoma

The human data prompted us to investigate the possibility that RANKL signaling contributes to primary

E-cadherin (E-cad)-positive, CD45-negative cells from KP tumors after 1 week of treatment with control Fc (n = 8) or RANK-Fc (n = 16). (*C*) Dot plot represents the percentage of phospho-Erk-positive area on lesions from KP mice treated over 1 week with control-Fc *(n = 27)* or RANK-Fc *(n = 116)*. (*D*) Tumor growth monitoring by μCT over an 8-week period. KP mice were treated during the last 6 weeks with control Fc or RANK-Fc. A total of 17 tumors were monitored for each treatment. Curves represent volume evolution of each tumor as fold of the first measurement. μCT imaging started 2 weeks before treatment initiation, and treatment started at week 0. Means with SE of the mean are shown in the box. (*A-D*) Statistical analyses were performed by using the Mann-Whitney test; asterisks show *p* values: **p* < 0.05, ***p* < 0.01, ****p* < 0.001.
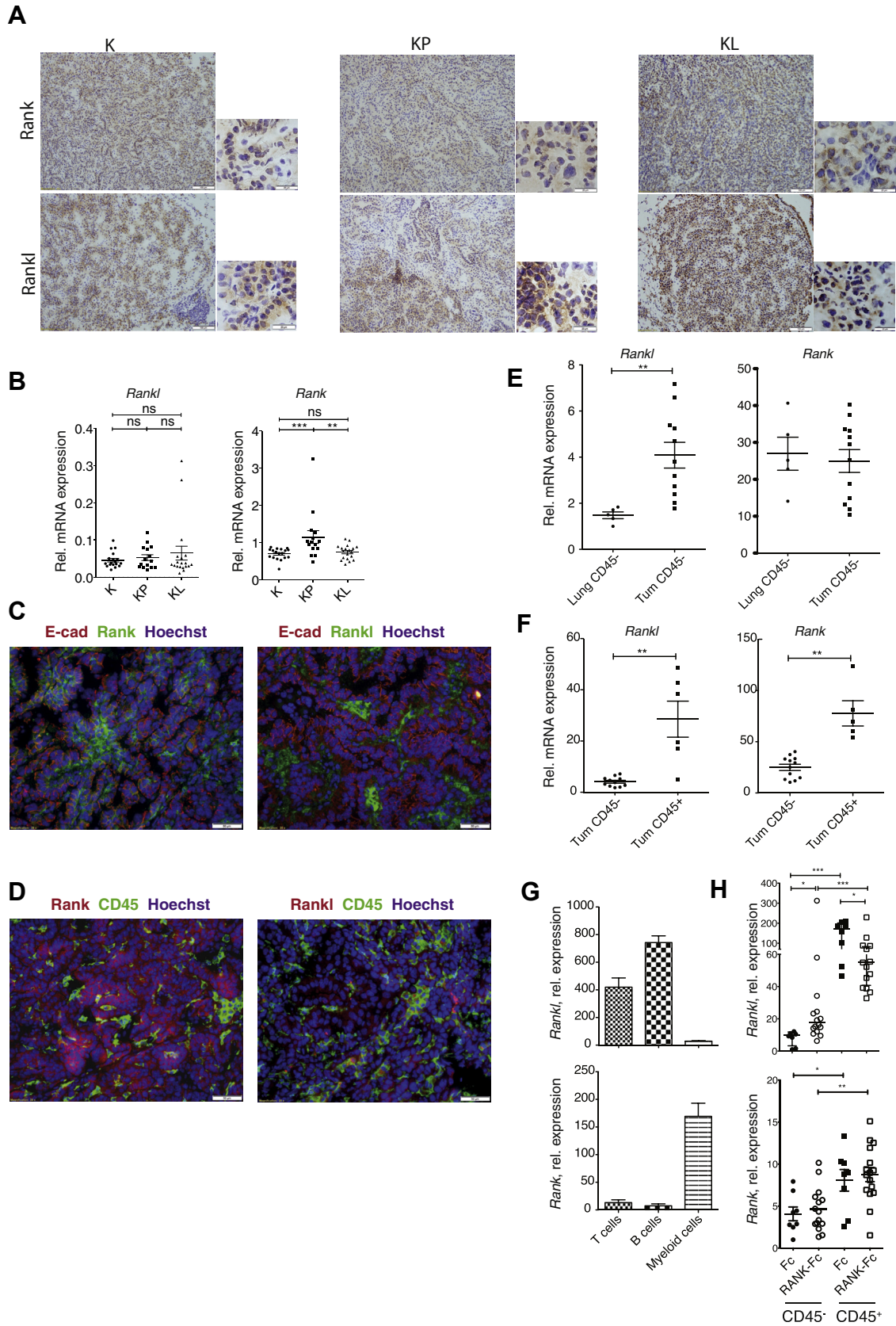
Figure 4. Tumor and immune cells differentially express receptor activator of NF-κB (Rank) ligand (Rankl) and Rank. (*A*) Immunohistochemistry pictures of frozen lung sections from tumor-bearing *K-ras$^{LSL-G12D/WT}$* (K), *Kras$^{LSL-G12D/WT}$; p53$^{FL/FL}$* (KP), or *Kras$^{LSL-G12D/WT}$; Lkb1$^{FL/FL}$* (KL) mice showing Rank (*top*) or Rankl (*bottom*) expression (*brown*) in tumors. Original magnification: large pictures, ×100; small pictures, ×500. (*B*) Dot plots show *Rankl* (*left*) and *Rank* (*right*) gene relative expression

tumor development in lung adenocarcinoma. To test this, we decided to block Rankl-Rank interaction with a recombinant protein composed of the extracellular portion of mouse RANK fused to human Fc (RANK-Fc), first in two genetically engineered mouse models of NSCLC, K-$ras^{LSL-G12D/WT}$ (designated as K hereafter) and K-$ras^{LSL-G12D/WT}$; $Lkb1^{FL/FL}$ (KL). In these models, tumor initiation is triggered in adult mice upon intratracheal delivery of viruses carrying the Cre recombinase, resulting in oncogenic $Kras(G12D)$ activation (K), or $Kras(G12D)$ activation concomitantly with deletion of tumor suppressor $Lkb1$ (KL). Loss of $Lkb1$ enables tumor progression toward aggressive adenocarcinoma, with transdifferentiation to squamous cell carcinoma in some cases.[19–21] For preclinical relevance, mice were treated with RANK-Fc or control Fc only when tumors were well established and visible by microcomputed tomography (μCT). Short-term (2 weeks for K and 1 week for KL mice) RANK-Fc treatment led to a significantly diminished tumor growth rate, with tumor shrinkage (i.e., relative growth <1) detected in multiple tumors, as monitored by μCT (Fig. 2A). This response was accompanied by a reduced proliferation of tumor cells (Ki67 staining) and reduced phospho-Erk, a marker of advanced grade in $Kras$-mutant lung tumors,[22,23] specifically in KL tumors. No change in apoptosis in K or KL tumors was observed, as assessed by cleaved caspase-3 staining (Fig. 2B–D). Next, to determine whether there is rapid tumor progression after initial sensitivity to Rankl inhibition, we treated the most aggressive model twice weekly with RANK-Fc or control Fc for a total duration of 3 weeks and monitored tumor growth rates longitudinally by μCT. Tumor growth remained compromised, indicating a durable response of primary lung adenocarcinoma to Rankl blockade (Fig. 2E). Hence, $Kras$-mutant lung tumors, whether expressing or not expressing $Lkb1$, are sensitive to Rankl blockade.

### Rankl Blockade Elicits Long-Term Antitumor Responses in K-$ras^{LSL-G12D/WT}$; $p53^{FL/FL}$ Mice

To evaluate the antitumor effects of Rankl blockade in yet another model, we treated tumor-bearing K-$ras^{LSL-G12D/WT}$; $p53^{FL/FL}$ (KP) mice[24] with RANK-Fc.

Similarly to the effect observed in K and KL mice, KP tumors were inherently sensitive to short-term Rankl blockade, although no change in tumor cell proliferation contrasting with that in KL tumors could be measured (Fig. 3A and B). Surprisingly, phospho-Erk was enhanced, suggesting a paradoxical Erk-dependent pathway activation in response to Rankl blocking therapy in KP tumors (Fig. 3C). A 6-week treatment follow-up indicated a long-term response to Rankl blockade in KP mice (Fig. 3D). Together, the results from Figures 2 and 3 demonstrate an inherent sensitivity and durable response to Rankl blockade in primary lung tumors in the mouse.

Rankl-Rank Expression Is Elevated in Tumor-Associated Immune Cells, but Blockade Does Not Lead to Major Changes in the Tumor Immune Microenvironment

Next, we decided to better characterize the effect of Rankl blockade. Staining of tumor sections by immunohistochemistry showed Rank and Rankl expression in each of the K, KP, and KL tumors (Fig. 4A). Monitoring by real-time polymerase chain reaction did not reveal any difference in $Rankl$ expression between the tumor genotypes, although there was stronger $Rank$ expression in KP than in K or KL tumors, thus contrasting with the human TCGA data (Fig. 4B). Immunofluorescence staining enabled us to detect each of Rank and Rankl plasma membrane protein expression heterogeneously within the tumor mass, with Rank frequently colocalizing with E-cadherin and Rankl with CD45-positive (immune) cells (Fig. 4C–D). To understand which cell types express $Rankl$ and $Rank$, we collected lung tumors or healthy lung from KP mice and used anti-CD45 magnetic beads to separate nonimmune (CD45-negative) from immune (CD45-positive) cells. This revealed a stronger expression of $Rankl$ in CD45-negative cells isolated from tumors (which consist mostly but not exclusively of tumor epithelial cells) than in CD45-negative cells from healthy lung, whereas $Rank$ expression was not different (Fig. 4E). In tumors, expression of $Rankl$ and $Rank$ was more elevated in immune than in nonimmune cells, with the strongest

---

from real-time polymerase chain reaction on K (n = 18), KP (n = 15), and KL (n = 19) tumors. (*C*) Representative immunofluorescence pictures showing Rank (*left*) or Rankl (*right*) in green together with E-cadherin (E-cad) (*red*) and Hoechst (*blue*) staining in KP tumors. (*D*) Representative immunofluorescence pictures showing Rank (*left*) or Rankl (*right*) in red together with CD45 (*green*) and Hoechst (*blue*) staining in KP tumors. (*C* and *D*) Original magnification, ×200. (*E*) *Rankl* and *Rank* relative mRNA expression from nonimmune (CD45-negative) cells of normal lung (n = 5) or KP tumors (n = 11). (*F*) *Rankl* and *Rank* relative mRNA expression of sorted CD45-negative (n = 11) or CD45-positive (n = 6) cells from KP tumors. (*G*) *Rankl* and *Rank* relative mRNA abundance in sorted CD3-positive T cells, B220-positive B cells, and CD3-negative B220-negative CD45-positive myeloid cells from KP tumors. Histograms represent the average of multiple experiments and error bars denote SE of the mean; n = 4, 4, and 7 experiments, respectively for T-cell, B-cell, and myeloid cell populations. (*H*) *Rankl* and *Rank* relative mRNA expression in CD45-negative and CD45-positive cells of tumors from control Fc or RANK-Fc treated KP mice. Treatment started at 23 weeks after tumor initiation, and duration was 2 weeks. (*B*, *E*, *F*, and *H*) Statistical analyses were performed by using the Mann-Whitney test. *p <0.05, **p <0.01, ***p < 0.001. Rel., relative; Tum, tumor.
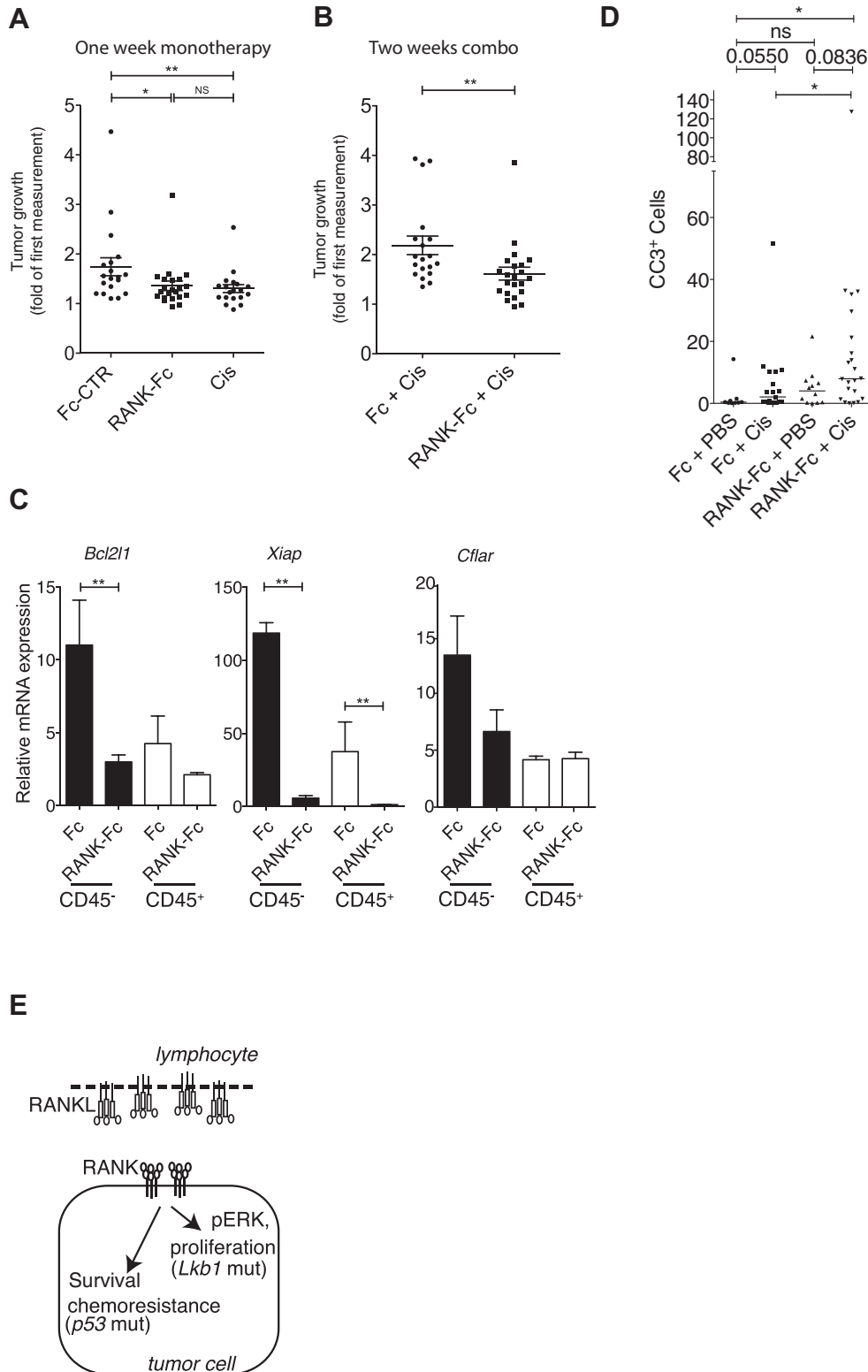
Figure 5. Receptor activator of NF-κB (Rank) ligand (Rankl) blockade increases chemotherapy efficacy in *Kras^{LSL-G12D/WT}*; *p53^{FL/FL}* (KP) tumors. (*A*) Dot plot shows tumor growth, determined by microcomputed tomography imaging, in KP mice treated or not during 1 week with Fc control (Fc-CTR) (n = 19), RANK-Fc (n = 22), or cisplatin (Cis) (n = 19). (*B*) Dot plot shows tumor growth, determined by microcomputed tomography imaging, in KP mice treated by a combination of control Fc (n = 19) or RANK-Fc (n = 22) plus Cis. Mice received Fc or RANK-Fc injections during a 2-week period plus one injection of Cis during the last week. (*C*) Relative mRNA abundance of the indicated genes in CD45-negative or CD45-positive sorted cells of tumors obtained from KP mice treated in (*B*). Error bars show SE of the mean. Statistical analyses comparing CD45-positive versus CD45-negative fractions were not performed. (*D*) Dot plot shows cleaved caspase-3-positive cell number per 10^6 pixels,

expression in B and T lymphocytes for *Rankl* and in myeloid cells for *Rank* (Fig. 4F–G). Because of this strong expression in immune cells within lung tumors, we next wanted to know whether treatment causes remodeling of the tumor immune microenvironment. RANK-Fc led to a significant increase in *Rankl* expression in nonimmune cells and a reduction in immune cells, whereas there was no perturbation in *Rank* expression (Fig. 4H). After 2 weeks of treatment, no change was observed in the proportion of B cells, whereas that of T lymphocytes diminished, which was not specific for any of the CD4-positive, T-regulatory, or CD8-positive subsets (Supplementary Fig. 2A–C). Rankl blockade did not result in any significant change in the expression of tumor necrosis factor gene (*Tnf*), interleukin 10 gene (*Il10*), or interferon gamma gene (*Ifng*) mRNAs in CD45-positive or CD45-negative cells and did not alter cytoplasmic expression of interferon gamma or tumor necrosis factor proteins in CD4-positive or CD8-positive T cells (Supplementary Fig. 2D and E). RANK was originally characterized in dendritic cells and suggested to participate in dendritic cell–dependent T-cell expansion, a hypothesis that was not supported by analysis of *Rank*-deficient mice.[3,4] Our results demonstrate that despite elevated Rank and Rankl expression in immune cells within the tumor microenvironment, Rankl blockade only marginally remodels the immune compartment, which does not support a major role for immune cells in the antitumor response.

Rankl Blockade Increases the Efficacy of Cisplatin Chemotherapy

To test the effect of combination treatment compared with monotherapy, we decided to treat tumor-bearing KP mice with RANK-Fc for 1 week followed by 1 week of standard chemotherapy cisplatin with maintenance of RANK-Fc and used μCT to compare tumor growth rates with those of tumors from mice treated with cisplatin alone. Short-term cisplatin caused a diminished tumor growth rate, as reported earlier,[25] which was not significantly different from RANK-Fc therapy (Fig. 5A). Combined RANK-Fc and cisplatin led to a more profound effect on tumor growth (Fig. 5B). When compared with cisplatin alone, combined therapy led to a significant decrease in the expression of the antiapoptotic genes Bcl-2-like protein 1 gene (*Bcl2l1*) and X-linked inhibitor of apoptosis gene (*Xiap*) in the tumor cell compartment,

as well as to *Xiap* in immune cells and increased apoptosis revealed by cleaved caspase-3 (Fig. 5C and D). In contrast, there was no additive effect of the combination treatment compared with that of chemotherapy alone in KL tumors, maybe because RANK-Fc diminishes tumor cell proliferation and hence does not favor success of an antiproliferative drug (Supplementary Fig. 3). Hence, our results highlight the efficacy of Rankl blockade in preclinical mouse models of lung adenocarcinoma. They suggest different mechanisms of action in different tumor molecular subtypes and that combination treatments will be more efficacious than chemotherapy alone in some but not all patients (Fig. 5E).

Bcl2l1 and *Xiap* are known NF-κB target genes. Signaling by NF-κB directly in the tumor epithelial cells plays an important role in the development of lung tumors in mouse models of NSCLC, notably in tumors initiated upon oncogenic *Kras* activation.[26–32] However, how the NF-κB pathway becomes activated in NSCLC is currently unclear. Because NF-κB most often responds to cell stimulation by extracellular ligands such as cytokines of the interleukin-1 or TNF families, one plausible scenario is that the tumor microenvironment triggers NF-κB activation in tumor cells by paracrine communication. As it is a potent activator of NF-κB, RANKL could participate in the elaboration of an NF-κB response in lung tumor cells.[15] Indeed, RANKL stimulates migration of the A549 human lung tumor cell line through the upregulation of the NF-κB target gene intercellular adhesion molecule 1 gene (*ICAM1*).[33] In future preclinical and clinical investigations, it will therefore be important to test whether RANKL participates in lung tumor development partly through NF-κB activation, and whether NF-κB targets could be used as biomarkers of denosumab treatment efficacy in patients' tumors.

In our study, we have used mouse models where tumor initiation depends on oncogenic *Kras* activation, because (1) *KRAS* is the most commonly mutated proto-oncogene in human NSCLC, (2) these models faithfully recapitulate many aspects of the development of the human disease, and (3) these models are refractory to many treatments and are thus relevant to assess new therapeutic opportunities (here Rankl blockade). Our preclinical results, combined with our bioinformatics analyses, depict a strong connection between mutant *KRAS* and RANKL signaling in lung adenocarcinoma, which probably does not take place in CRC. Hence, our

---

in KP mice treated as in (*B*). Control-Fc plus phosphate-buffered saline (PBS) (n = 10), control-Fc plus Cis (n = 19), RANK-Fc + PBS (n = 12), and RANK-Fc plus Cis (n = 22). (*E*) Model of RANKL signaling in lung tumor cells. In *p53*-deficient tumors, the response to Rankl blockade is additive with Cis, resulting in decreased tumor cell survival. In liver kinase B1 gene (*Lkb1*)-deficient tumors, Rankl blockade inhibits Erk activity and tumor cell proliferation. (*A-D*) Statistical analyses were performed by using Mann-Whitney test. Asterisks show statistical *p* values: *$p < 0.05$, **$p < 0.01$. ns, not significant; pERK, phospho-ERK; mut, mutated; *Bcl2l1*, Bcl-2-like protein 1 gene; *Xiap*, X-linked inhibitor of apoptosis gene; *Cflar*, CASP8 and FADD like apoptosis regulator gene.

observations are generating the hypothesis that RANKL blockade will be efficient in *KRAS*-mutant lung tumors. An important future step will be to verify this hypothesis directly in tumor samples from patients.

Case Report of a Patient with Stage IV NSCLC Treated with Denosumab Monotherapy

A female patient, who was a former smoker with a 30-pack-year smoking history, presented with a middle lobe lung adenocarcinoma, *EGFR* WT, without anaplastic lymphoma receptor tyrosine kinase gene (*ALK*) rearrangement, cT4 cN0 cM1b (lower right lobe and bone metastases in the thoracolumbar spine especially L3, pelvis, femoral collar) stage IV. The adenocarcinoma was diagnosed on March 15, 2013 (by a transbronchial biopsy lower right lobe). The patient was hesitant regarding chemotherapy. Although she was presenting several painful bone metastases, an initial treatment of denosumab monotherapy was introduced as the first step in her oncology management, in parallel with supportive care including lumbar spine palliative radiotherapy in March. She decided to start chemotherapy on May 21, which was 2 months after the diagnosis. A new computed tomography scan was performed before she started undergoing chemotherapy, 4 weeks after a unique cycle of denosumab only, showing a primary lung tumor partial response (Fig. 6A and B). Thereafter, she received systemic chemotherapy (10 cycles [four platinum-pemetrexed and 6 pemetrexed], with partial response and thereafter with stable disease). She died 7 months after diagnosis.

This clinical case illustrates the potential efficacy, at least in select cases, of RANKL blockade therapy, even in advanced disease as monotherapy. Furthermore, the very large unplanned retrospective analysis of denosumab versus zoledronic acid in bone metastatic lung cancer[16] and our gene expression data set analyses of human lung adenocarcinoma both support the hypothesis of an improved OS. The activity of denosumab as an antineoplastic drug for the treatment of advanced NSCLC in combination with frontline platinum-based chemotherapy is currently being evaluated in the large randomized phase 3 European Organization for Research and Treatment of Cancer/European Thoracic Oncology Platform trial SPLENDOUR, with a primary end point of OS and a parallel retrospective analysis of RANK signaling pathway activation, including RANK and RANKL expression at baseline for all patients.

Acknowledgments
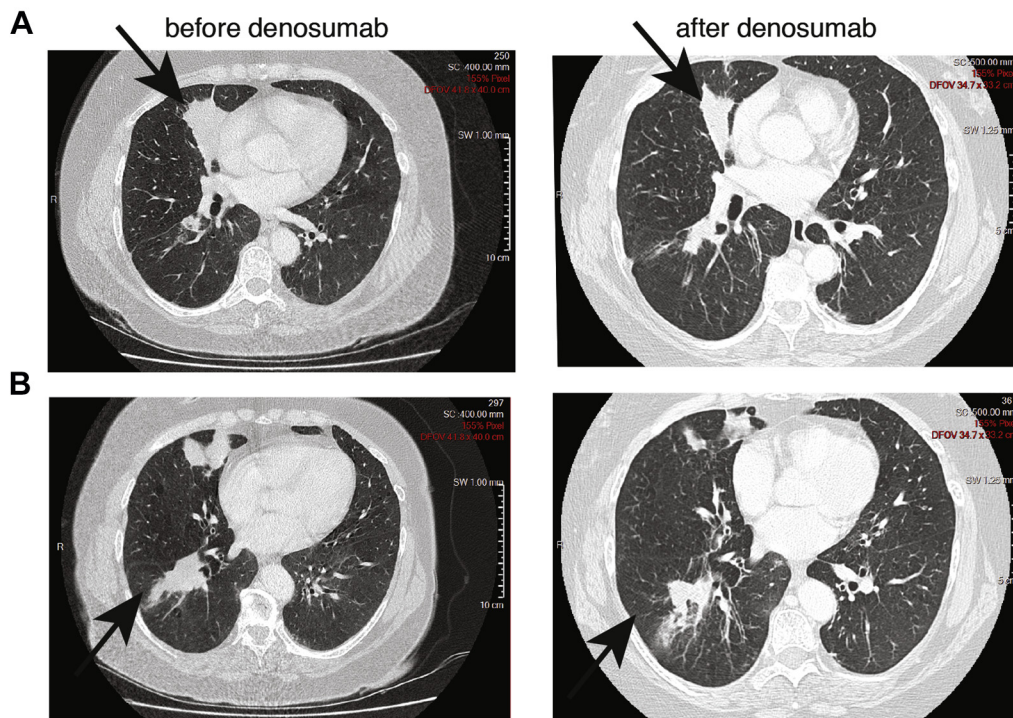
Figure 6. Clinical efficacy of denosumab monotherapy in a patient with NSCLC. (*A* and *B*) Computed tomography scans of the thorax of a chemotherapy-naive patient with stage IV NSCLC showing middle lobe adenocarcinoma (*A*) and a lower lobe secondary lesion (*B*) before (*left*) and after (*right*) a single dose of denosumab, demonstrating a significant partial response 4 weeks after a single infusion.

Supplementary Data

Note: To access the supplementary material accompanying this article, visit the online version of the *Journal of Thoracic Oncology* at www.jto.org and at https://doi.org/10.1016/j.jtho.2017.11.121.

References

1. Ferlay J, Soerjomataram I, Dikshit R, et al. Cancer incidence and mortality worldwide: sources, methods and major patterns in GLOBOCAN 2012. *Int J Cancer*. 2015;136:E359-E386.
2. Morgensztern D, Campo MJ, Dahlberg SE, et al. Molecularly targeted therapies in non-small-cell lung cancer annual update 2014. *J Thorac Oncol*. 2015;10:S1-S63.
3. Anderson DM, Maraskovsky E, Billingsley WL, et al. A homologue of the TNF receptor and its ligand enhance T-cell growth and dendritic-cell function. *Nature*. 1997;390:175-179.
4. Dougall WC, Glaccum M, Charrier K, et al. RANK is essential for osteoclast and lymph node development. *Genes Dev*. 1999;13:2412-2424.
5. Fata JE, Kong YY, Li J, et al. The osteoclast differentiation factor osteoprotegerin-ligand is essential for mammary gland development. *Cell*. 2000;103:41-50.
6. Kong YY, Yoshida H, Sarosi I, et al. OPGL is a key regulator of osteoclastogenesis, lymphocyte development and lymph-node organogenesis. *Nature*. 1999;397:315-323.
7. Jones DH, Nakashima T, Sanchez OH, et al. Regulation of cancer cell migration and bone metastasis by RANKL. *Nature*. 2006;440:692-696.
8. Zhang J, Dai J, Qi Y, et al. Osteoprotegerin inhibits prostate cancer-induced osteoclastogenesis and prevents prostate tumor growth in the bone. *J Clin Invest*. 2001;107:1235-1244.
9. Tan W, Zhang W, Strasner A, et al. Tumour-infiltrating regulatory T cells stimulate mammary cancer metastasis through RANKL-RANK signalling. *Nature*. 2011;470:548-553.
10. Gonzalez-Suarez E, Jacob AP, Jones J, et al. RANK ligand mediates progestin-induced mammary epithelial proliferation and carcinogenesis. *Nature*. 2010;468:103-107.
11. Schramek D, Leibbrandt A, Sigl V, et al. Osteoclast differentiation factor RANKL controls development of progestin-driven mammary cancer. *Nature*. 2010;468:98-102.
12. Tanos T, Sflomos G, Echeverria PC, et al. Progesterone/RANKL is a major regulatory axis in the human breast. *Sci Transl Med*. 2013;5:182ra155.
13. Palafox M, Ferrer I, Pellegrini P, et al. RANK induces epithelial-mesenchymal transition and stemness in human mammary epithelial cells and promotes tumorigenesis and metastasis. *Cancer Res*. 2012;72:2879-2888.
14. Henry DH, Costa L, Goldwasser F, et al. Randomized, double-blind study of denosumab versus zoledronic acid in the treatment of bone metastases in patients with advanced cancer (excluding breast and prostate cancer) or multiple myeloma. *J Clin Oncol*. 2011;29:1125-1132.
15. Peters S, Meylan E. Targeting receptor activator of nuclear factor-kappa B as a new therapy for bone metastasis in non-small cell lung cancer. *Curr Opin Oncol*. 2013;25:137-144.
16. Scagliotti GV, Hirsh V, Siena S, et al. Overall survival improvement in patients with lung cancer and bone metastases treated with denosumab versus zoledronic acid: subgroup analysis from a randomized phase 3 study. *J Thorac Oncol*. 2012;7:1823-1829.
17. Shepherd FA, Domerg C, Hainaut P, et al. Pooled analysis of the prognostic and predictive effects of KRAS mutation status and KRAS mutation subtype in early-stage resected non-small-cell lung cancer in four trials of adjuvant chemotherapy. *J Clin Oncol*. 2013;31:2173-2181.
18. Skoulidis F, Byers LA, Diao L, et al. Co-occurring genomic alterations define major subsets of KRAS-mutant lung adenocarcinoma with distinct biology, immune profiles, and therapeutic vulnerabilities. *Cancer Discov*. 2015;5:860-877.
19. Han X, Li F, Fang Z, et al. Transdifferentiation of lung adenocarcinoma in mice with Lkb1 deficiency to squamous cell carcinoma. *Nat Commun*. 2014;5:3261.
20. Jackson EL, Willis N, Mercer K, et al. Analysis of lung tumor initiation and progression using conditional expression of oncogenic K-ras. *Genes Dev*. 2001;15:3243-3248.
21. Ji H, Ramsey MR, Hayes DN, et al. LKB1 modulates lung cancer differentiation and metastasis. *Nature*. 2007;448:807-810.
22. Feldser DM, Kostova KK, Winslow MM, et al. Stage-specific sensitivity to p53 restoration during lung cancer progression. *Nature*. 2010;468:572-575.
23. Junttila MR, Karnezis AN, Garcia D, et al. Selective activation of p53-mediated tumour suppression in high-grade tumours. *Nature*. 2010;468:567-571.
24. Jackson EL, Olive KP, Tuveson DA, et al. The differential effects of mutant p53 alleles on advanced murine lung cancer. *Cancer Res*. 2005;65:10280-10288.
25. Oliver TG, Mercer KL, Sayles LC, et al. Chronic cisplatin treatment promotes enhanced damage repair and tumor progression in a mouse model of lung cancer. *Genes Dev*. 2010;24:837-852.
26. Barbie DA, Tamayo P, Boehm JS, et al. Systematic RNA interference reveals that oncogenic KRAS-driven cancers require TBK1. *Nature*. 2009;462:108-112.

27. Basseres DS, Ebbs A, Levantini E, Baldwin AS. Requirement of the NF-kappaB subunit p65/RelA for K-Ras-induced lung tumorigenesis. *Cancer Res*. 2010;70:3537–3546.

28. Duran A, Linares JF, Galvez AS, et al. The signaling adaptor p62 is an important NF-kappaB mediator in tumorigenesis. *Cancer Cell*. 2008;13:343–354.

29. Meylan E, Dooley AL, Feldser DM, et al. Requirement for NF-kappaB signalling in a mouse model of lung adeno-carcinoma. *Nature*. 2009;462:104–107.

30. Stathopoulos GT, Sherrill TP, Cheng DS, et al. Epithelial NF-kappaB activation promotes urethane-induced lung carcinogenesis. *Proc Natl Acad Sci U S A*. 2007;104:18514–18519.

31. Xia Y, Yeddula N, Leblanc M, et al. Reduced cell prolif-eration by IKK2 depletion in a mouse lung-cancer model. *Nat Cell Biol*. 2012;14:257–265.

32. Xue W, Meylan E, Oliver TG, et al. Response and resis-tance to NF-kappaB inhibitors in mouse models of lung adenocarcinoma. *Cancer Discov*. 2011;1:236–247.

33. Chen LM, Kuo CH, Lai TY, et al. RANKL increases migra-tion of human lung cancer cells through intercellular adhesion molecule-1 up-regulation. *J Cell Biochem*. 2011;112:933–941.